OPTIMIZATION OF COMPACT SYNCHROTRON OPTICS FOR X-RAY LITHOGRAPHY*

G. A. Decker, B. C. Craft
Brookhaven National Laboratory
Upton, N.Y. 11973

Abstract

The production of integrated circuits having sub-micron component dimensions has motivated the development of compact electron storage rings to provide synchrotron x-ray radiation [1-9]. This paper presents considerations for optimizing the optics for small radius rings using superconducting dipole magnets. The key parameters are the sizes and angular divergences of the source points illuminating the different ports. Two ring designs are compared in terms of theoretical beam parameters achievable using idealized optics.

Background

The horizontal beam size σ_x and angular divergence $\sigma_{x'}$ in a storage ring are given by

$$\sigma_x(s) = [\,\beta_x(s)\,\epsilon_x + (\,\eta(s)\,\sigma_\epsilon)^2\,]^{1/2} \qquad (1)$$

and

$$\sigma_{x'}(s) = \left[\frac{1+\alpha_x^2(s)}{\beta_x(s)}\epsilon_x + (\,\eta'(s)\,\sigma_\epsilon)^2\right]^{1/2} \qquad (2)$$

There are contributions from the emittance ϵ_x and the rms energy spread σ_ϵ. The horizontal beta function β_x, the dispersion function η, and $\alpha_x \equiv -\beta_x'/2$ are in general dependent on the longitudinal coordinate, s. This dependence leads to differing source characteristics at the various light extraction ports around the ring.

Initial studies conducted by lithographers [6] indicate that the desired limits on horizontal spot size and divergence are roughly

$$\sigma_x \leq 1mm \quad \text{and} \quad \sigma_{x'} \leq 1mr. \qquad (3)$$

The desired critical wavelength of the source is taken to be $\lambda_c = 10A$.

Cylindrically Symmetric Design

The cylindrically symmetric ring design [1,8] is characterized by critical wavelength λ_c, dipole field strength B, and horizontal field gradient index n as defined by

$$n = -\frac{\rho}{B}\frac{\partial B}{\partial x}, \qquad (4)$$

where ρ is the radius of curvature. The horizontal rms beam size and angular divergence for this design are given by

$$\sigma_x = 19.8\ \lambda_c^{-3/4}\ B^{-5/4}\left[\frac{1}{n(1-n)} + \frac{1}{(1-n)(3-4n)}\right]^{1/2} \qquad (5)$$

and

$$\sigma_{x'} = 1.38\ \lambda_c^{-1/4}\ B^{1/4}\left[\frac{1}{n}\right]^{1/2} \qquad (6)$$

For λ_c in units of angstroms and B in units of Tesla, σ_x and $\sigma_{x'}$ are in units of millimeters and milliradians, respectively.

An interesting feature of Eqs. (5) and (6) is that dimensional parameters λ_c and B have been separated from the dimensionless geometrical factors involving n. In general, the geometrical factors would be more complex expressions involving focal lengths of quadrupoles and drift lengths, but the overall factor would be dimensionless (see Appendix A). This clearly indicates the effects of varying λ_c and B. As λ_c is decreased, both spot size and beam divergence increase. Though a cylindrical machine may produce acceptable spot characterstics at $\lambda_c = 20A$, the original Klein-ERNA design value [1], both spot size and divergence are at best marginal, in the absence of coupling, when scaled to $\lambda_c = 10A$.

As the field strength B is reduced, the beam divergence improves slightly but the spot size increases significantly. Machine designs utilizing conventional dipoles can counteract this $B^{-5/4}$ dependency of the beam size only by resorting to more complicated geometries.

Symmetric Racetrack Design

The lattice considered here has two 180° dipoles with uniform and equal field index which are connected by straight sections, containing quadrupoles and drifts, which are symmetric about their midpoints. Besides allowing several mathematical simplifications due to symmetry, this lattice is expected to produce a local minimum of emittance in parameter space.

For the purpose of optimization, three different functions-of-merit are considered. In order to take advantage of the scaling properties indicated in Appendix A, the functions chosen maintain the homogeneity of the scaling parameters. Explicitly, the functions used are

$$\langle\tilde{\sigma}_x\rangle\langle\tilde{\sigma}_{x'}\rangle\ ,\ \langle\tilde{\sigma}_x\rangle\langle\tilde{\sigma}_{x'}\rangle^5\ ,\ \text{and}\ \ \tilde{\sigma}_x(0°) \qquad (7)$$

where $\tilde{\sigma}_x$ and $\tilde{\sigma}_{x'}$ are dimensionless quantities. The source size and divergence are calculated by multiplying these quantities by

$$l \equiv \gamma\sqrt{C_q\,\rho} \quad \text{and} \quad \theta \equiv \gamma\sqrt{C_q/\rho}$$

respectively. Here $\langle\ \rangle$ means average over port locations at 0°, ±20°, and ±40° in the dipole. The third form indicates a single point sample at the center of the dipole. From Eqs. (1) and (2), these functions depend on the betatron and dispersion functions, their derivatives and the longitudinal and horizontal emittances. The beta function in the dipole of a lattice with the assumed symmetry depends only on β_0, the value in the center of the dipole, and n. Similarly, the dispersion function depends only on η_0 and n. With parameterizations of β and η in the dipoles, the emittances can be calculated. The above functions-of-merit, referred to generically by F_m, can therefore be written as

$$F_m = F_m(\beta_0\ ,\ \eta_0\ ,\ n\ ). \qquad (8)$$

As shown in the first half of Appendix B, the phase advance through the straight section is determined by the values of the betatron and dispersion functions and their derivatives at the exit of the dipole. Since the horizontal phase advance through the dipole depends only on β_0 and n, the horizontal tune can be written as

$$\nu_x = \nu_x(\beta_0\ ,\ \eta_0\ ,\ n\ ). \qquad (9)$$

Since the tune of a storage ring is a critical operating parameter, it is desirable to have it be an independent rather than dependent variable during the optimization process. Eq. (9) can be rewritten to give

$$\eta_0 = \eta_0(\nu_x\ ,\ \beta_0\ ,\ n\ ). \qquad (10)$$

This can be substituted in Eq. (8) to yield

$$F_m = F_m(\nu_x\ ,\ \beta_0\ ,\ n\ ). \qquad (11)$$

Using the first form in Eq. (7), the behavior of Eq. (11) for $\nu_x = 1.4$ is shown in Figure 1 where contours are spaced by 0.1. Table 1 indicates the dependence of the optimization on ν_x and details the resulting normalized beam spot characteristics.

Considering now the dipole strength, Eqs. (A.10) and (A.11) show that increasing B improves the value of the function-of-merit indefinitely but at the expense of $\sigma_{x'}$. The value of $B = 3.5$ Tesla satisfies the lithographer's requirements as stated in Eqs. (3). The radius of curvature for $\lambda_c = 10A$ is then 0.69 meters and the resultant source characteristics for $\nu_x = 1.4$, in the absence of coupling, are tabulated in Table 2.

* Research supported by the U.S. Department of Energy

CH2387-9/87/0000-0464 $1.00 © IEEE

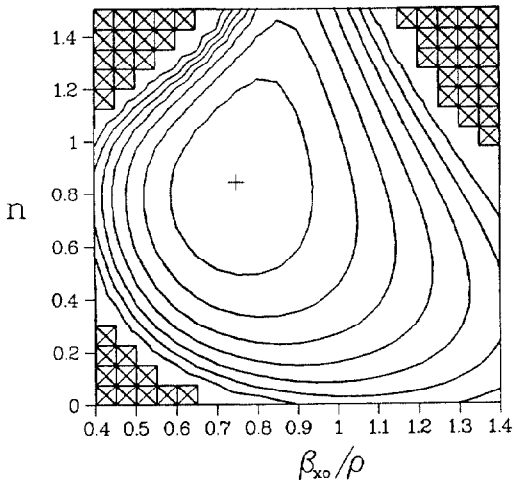

Figure 1. Dependence of F_m on β_0 and n

Table 1. Dependence of F_m on ν_z

ν_z	n	$\frac{\beta}{\rho}$	$\frac{\eta}{\rho}$	0°		40°		F_m
				$\bar{\sigma}_z$	$\bar{\sigma}_{z'}$	$\bar{\sigma}_z$	$\bar{\sigma}_{z'}$	
1.05	0.74	1.32	1.02	1.36	0.79	1.51	0.88	1.20
1.10	0.75	1.27	0.89	1.23	0.77	1.40	0.87	1.08
1.15	0.77	1.20	0.77	1.11	0.76	1.29	0.87	0.98
1.20	0.79	1.11	0.66	1.00	0.75	1.20	0.88	0.90
1.25	0.81	1.02	0.57	0.91	0.76	1.12	0.89	0.83
1.30	0.82	0.93	0.50	0.82	0.77	1.05	0.90	0.78
1.35	0.83	0.84	0.44	0.75	0.78	0.99	0.92	0.74
1.40	0.84	0.75	0.39	0.68	0.80	0.95	0.94	0.72
1.45	0.85	0.67	0.36	0.63	0.83	0.92	0.97	0.70
1.50	0.86	0.59	0.33	0.58	0.88	0.91	1.00	0.70
1.55	0.86	0.51	0.31	0.54	0.93	0.90	1.05	0.72
1.60	0.86	0.45	0.29	0.50	1.00	0.92	1.10	0.76
1.65	0.86	0.38	0.28	0.47	1.09	0.95	1.18	0.83
1.70	0.86	0.32	0.27	0.45	1.22	1.01	1.30	0.94
1.75	0.87	0.26	0.27	0.43	1.41	1.12	1.47	1.15

Table 2. Source size for ν_z =1.4

Port Angle	σ_z (mm)	$\sigma_{z'}$ (mr)
0°	0.50	0.85
20°	0.56	0.89
40°	0.70	1.00

To complete the design, the straight sections must be developed and the vertical tune considered. From Appendix B, if a triplet is used to match the horizontal machine functions, two of the four parameters defining the straight section, l_1, l_2, f_1, f_2, remain free parameters. Imposing a constraint on the vertical tune leaves only one. Taking l_1 to be the free parameter determined by the cryostat of the dipole and injection considerations, a value of 0.5m is assumed. For B=3.5T and ν_z=1.4, fixing ν_y=1.4 yields l_2=1.22m, f_1=.88m. and f_2=1.79m. The resultant orbital circumference is 11.2m.

Conclusions

The cylindrical design is marginal in its performance with respect to the requirements of x-ray lithographers as stated above. Although coupling can improve the low current source characteristics, current-dependent effects such as anomalous bunch lengthening will certainly degrade performance. The symmetric racetrack, besides allowing independent tune control and relative simplicity in implementation of rf and injection, satisfies the lithography requirements without coupling.

Appendix A: Scaling

Here the source size and angular divergence are shown to scale in a simple way with radius of curvature ρ and beam energy γ. Using the notation of [10], the differential equations for the betatron and dispersion functions are

$$\frac{1}{2}\beta\beta'' - \frac{1}{4}\beta'^2 + K\beta^2 = 1 \qquad \text{(A.1)}$$

and

$$\eta'' = K\eta + G \qquad \text{(A.2)}$$

where G specifies the dipole field strength and has units of m^{-1} and K describes the quadrupole strength and has units of m^{-2}. If ρ is scaled, then G scales like ρ^{-1} and K scales like ρ^{-2}. Since differentiation with respect to s scales like ρ^{-1}, inspection of Eqs. (A.3) and (A.4) indicates that β and η scale like ρ.

Considering next the damping partition numbers given by

$$J_x = 1-D \quad \text{and} \quad J_\epsilon = 2+D \ , \qquad \text{(A.3)}$$

where

$$D = \frac{\int \eta G\,(G^2+2K)\,ds}{\int G^2 ds} \ , \qquad \text{(A.4)}$$

it is clear they are independent of scaling ρ. Consequently the relative energy spread or longitudinal emittance

$$\sigma_\epsilon = \left[\frac{C_q\,\gamma^2 <G^3>}{J_\epsilon <G^2>}\right]^{1/2} \qquad \text{(A.5)}$$

where C_q is a constant [10], scales like $\rho^{-1/2}$. Similarly, the horizontal emittance given by

$$\epsilon_x = \frac{C_q\,\gamma^2 <G^3 H>}{J_x <G^2>} \qquad \text{(A.6)}$$

where

$$H = \frac{1}{\beta}\left[\eta^2 + \left(\beta\eta' - \frac{\beta'\eta}{2}\right)^2\right] \qquad \text{(A.7)}$$

can been seen to be independent of scaling ρ.

Combining the above results and referring to Eqs. (1) and (2) in the main text leads to the deduction that σ_z scales like $\rho^{1/2}$ and $\sigma_{z'}$ scales like $\rho^{-1/2}$. Considering again Eqs. (A.3) and (A.4) one finds that both σ_z and $\sigma_{z'}$ scale like γ as the energy is varied. These results can be summerized by

$$\sigma_z = \sqrt{C_q\rho}\ \gamma\ \mathbf{F}(lattice) \qquad \text{(A.8)}$$

and

$$\sigma_{z'} = \sqrt{C_q/\rho}\ \gamma\ \mathbf{G}(lattice) \qquad \text{(A.9)}$$

where the dimensionless functions **F** and **G** reflect the geometric properties of the lattice independent of the electron energy and the scale of the bending radius.

The utility of Eqs. (A.8) and (A.9) is realized when lattice design optimization is considered. For a useful class of functions-of-merit, the above factorization effectively reduces the dimensionality of the parameter space by two because the lattice geometry, represented by **F** and **G**, can be optimized independent of ρ and γ. Useful alternatives to Eqs. (A.8) and (A.9) can be realized by expressing ρ and γ in terms of λ_c and the main dipole field strength B. This results in the proportionalities

$$\sigma_z \propto \lambda_c^{-3/4} B^{-5/4} \qquad \text{(A.10)}$$

and

$$\sigma_{z'} \propto \lambda_c^{-1/4} B^{1/4} \qquad \text{(A.11)}$$

In this form, the constraint on λ_c is trivially imposed and the effect of varying the dipole field strength is shown.

Appendix B: Matching

Matching, the design of an optical transport system using quadrupole focusing elements and drift spaces, is a common practice in lattice design. In this appendix, two examples particularly relevant to the design of symmetric racetrack machines are

presented. If R is used to represent the linear transport matrix that takes x and x' from location 1 to location 2, then the betatron and dispersion functions evolve according to

$$\beta_2 = R_{11}^2\ \beta_1 - 2\,R_{11}\,R_{12}\,\alpha_1 + R_{12}^2\ \frac{1+\alpha_1^2}{\beta_1}\ , \qquad \text{(B.1)}$$

$$\eta_2 = R_{11}\,\eta_1 + R_{12}\,\eta_1' \ . \qquad \text{(B.2)}$$

Taking locations 1 and 2 to be at the beginning and end, respectively, of the straight section in a symmetric racetrack lattice implies that $\beta_2 = \beta_1$ and $\eta_2 = \eta_1$. Using this and dropping the subscript 1, Eqs. (B.1) and (B.2) become

$$R_{11} = 1 - \frac{\eta'}{\eta}\,R_{12}\ , \qquad \text{(B.3)}$$

$$(R_{11}^2 - 1)\,\beta - 2R_{11}R_{12}\alpha + R_{12}^2\ \frac{1+\alpha^2}{\beta} = 0\ . \qquad \text{(B.4)}$$

The betatron phase advance through the symmetric straight section can be shown [11] to be given by

$$\sin(\delta\phi) = \frac{R_{12}}{\beta}\ . \qquad \text{(B.5)}$$

Combining Eqs. (B.3) and (B.4) to eliminate R_{11} and substituting into Eq. (B.5) yields, upon trigonometric simplification

$$\tan(\frac{\delta\phi}{2}) = \frac{\eta'}{\eta}\beta + \alpha\ . \qquad \text{(B.6)}$$

This result implies that it is impossible to construct a straight section, regardless of complexity, that allows adjustment of the horizontal tune without affecting the horizontal betatron and dispersion functions in the dipoles.

As a second, more practical example of matching, consider matching a triplet into the straight section of a symmetric racetrack. To achieve a "match", the betatron and dispersion functions are developed from one end of the straight section and the constraint that their derivatives vanish in the center of the straight is imposed. This results in functional relationships between drift lengths, quadrupole focal lengths, and the machine functions desired at the ends of the straight section.

The specific case considered is indicated by the following thin-lens matrix representation R for the first half of the straight section.

$$R = \begin{pmatrix} 1 & 0 \\ 1/f_2 & 1 \end{pmatrix}\begin{pmatrix} 1 & l_2 \\ 0 & 1 \end{pmatrix}\begin{pmatrix} 1 & 0 \\ -1/f_1 & 1 \end{pmatrix}\begin{pmatrix} 1 & l_1 \\ 0 & 1 \end{pmatrix} \qquad \text{(B.7)}$$

The derivatives of the machine functions evolve according to

$$\alpha_2 = -R_{11}R_{21}\beta_1 + (1 + 2R_{12}R_{21})\alpha_1 \qquad \text{(B.8)}$$

$$-R_{12}R_{22}\,\frac{1+\alpha_1^2}{\beta_1}$$

and

$$\eta_2' = R_{21}\eta_1 + R_{22}\eta_1' \ . \qquad \text{(B.9)}$$

Imposing the condition $\eta_2' = 0$ and $\alpha_2 = 0$ reduces equations B.8 and B.9 to

$$f_2 = \frac{f_1}{(1 - \frac{f_1}{\eta/\eta' + l_1})} - l_2 \qquad \text{(B.10)}$$

and

$$f_1 = \frac{(\beta - l_1\alpha)t - l_1}{(\beta - (l_1+l_2)\alpha)t - (l_1+l_2)}\ l_2 \qquad \text{(B.11)}$$

where the abbreviation $t = \tan(\delta\phi/2)$ has been used. The subscript 1 on the machine functions entering the straight section has been dropped.

Eqs. (B.10) and (B.11) describe the correlation between focal lengths and drift space lengths required to achieve a match into the horizontal machine functions inside the dipoles. Two of the parameters are constrained by the match and two remain free.

References

[1] U. Trinks, F. Nolden and A. Jahnke, "The table-top synchrotron radiation source *Klein-ERNA*," Nuclear Instruments and Methods, vol. 200, pp. 475-479, 1982.

[2] A. Heuberger, "Comparison of different x-ray sources: X-ray tubes, laser induced plasma sources, compact and conventional storage rings," in Proceedings of the SPIE, vol. 448, 1983, p.8.

[3] Y. Miyahara, K. Takata and T. Nakanishi, "Superconducting racetrack electron storage ring and coexistent injector microtron for synchrotron radiation," ISSP TR B-12, University of Tokyo, September 1984.

[4] Proceedings of Workshop on Compact Storage Ring Technology: Application to Lithography, BNL 52005, 1986.

[5] Report of the Second Workshop on Synchrotron Radiation Sources For X-ray Lithography, BNL 38789, 1986

[6] W. D. Klotz, et al., "The use of superconductivity in compact storage rings," presented at the Eleventh International Cryogenic Engineering Conference, Berlin, West Germany, 1986.

[7] C. Mileikowsky, "The microtron in x-ray lithography," presented at the Ninth International Conference on the Application of Accelerators to Research and Industry, Denton, Texas, November 10-12, 1986.

[8] N. Takahashi, "Compact superconducting SR ring for x-ray lithography," presented at the Ninth International Conference on the Application of Accelerators to Research and Industry, Denton, Texas, November 10-12, 1986.

[9] Report of the Third Workshop Program for X-ray Lithography Development, BNL 52046,1986.

[10] M. Sands, "The physics of electron storage rings: An introduction," SLAC-121, UC-28 (ACC), University of California at Santa Cruz, November 1970.

[11] K. L. Brown and R. V. Servranckx, "First- and second-order charged particle optics," in AIP Conference Proceedings, No. 127, 1983, pp. 62-138.